UNIVERSITÉ DE GENÈVE

Archive ouverte UNIGE
https://archive-ouverte.unige.ch

Article scientifique | Article | 2007

Published version | Open Access

This is the published version of the publication, made available in accordance with the publisher's policy.

Transdermal delivery of cytochrome C--A 12.4 kDa protein--across intact skin by constant-current iontophoresis

Cazares Delgadillo, Jennyfer; Naik, Aarti; Ganem-Rondero, A; Quintanar-Guerrero, D; Kalia, Yogeshvar

How to cite

CAZARES DELGADILLO, Jennyfer et al. Transdermal delivery of cytochrome C--A 12.4 kDa protein--across intact skin by constant-current iontophoresis. In: Pharmaceutical research, 2007, vol. 24, n° 7, p. 1360–1368. doi: 10.1007/s11095-007-9294-4

This publication URL: https://archive-ouverte.unige.ch/unige:22651

Publication DOI: 10.1007/s11095-007-9294-4

© This document is protected by copyright. Please refer to copyright holder(s) for terms of use.

Pharmaceutical Research, Vol. 24, No. 7, July 2007 (© 2007)
DOI: 10.1007/s11095-007-9294-4

Research Paper

Transdermal Delivery of Cytochrome C—A 12.4 kDa Protein—Across Intact Skin by Constant–Current Iontophoresis

J. Cázares-Delgadillo,[1,2] A. Naik,[1,2,4] A. Ganem-Rondero,[3] D. Quintanar-Guerrero,[3] and Y. N. Kalia[1,2,5]

Received December 10, 2006; accepted March 12, 2007; published online April 25, 2007

Purpose. To demonstrate the transdermal iontophoretic delivery of a small (12.4 kDa) protein across intact skin.

Materials and Methods. The iontophoretic transport of Cytochrome c (Cyt c) across porcine ear skin *in vitro* was investigated and quantified by HPLC. The effect of protein concentration (0.35 and 0.7 mM), current density (0.15, 0.3 or 0.5 $mA.cm^{-2}$ applied for 8 h) and competing ions was evaluated. Co-iontophoresis of acetaminophen was employed to quantify the respective contributions of electromigration (EM) and electroosmosis (EO).

Results. The data confirmed the transdermal iontophoretic delivery of intact Cyt c. Electromigration was the principal transport mechanism, accounting for ~90% of delivery; correlation between EM flux and electrophoretic mobility was consistent with earlier results using small molecules. Modest EO inhibition was observed at 0.5 $mA.cm^{-2}$. Cumulative permeation at 0.3 and 0.5 $mA.cm^{-2}$ was significantly greater than that at 0.15 $mA.cm^{-2}$; fluxes using 0.35 and 0.7 mM Cyt c in the absence of competing ions ($J_{tot} = 182.8 \pm 56.8$ and 265.2 ± 149.1 $\mu g.cm^{-2}.h^{-1}$, respectively) were statistically equivalent. Formulation in PBS (pH 8.2) confirmed the impact of competing charge carriers; inclusion of ~170 mM Na^+ resulted in a 3.9-fold decrease in total flux.

Conclusions. Significant amounts (~0.9 $mg.cm^{-2}$ over 8 h) of Cyt c were delivered non-invasively across intact skin by transdermal electrotransport.

KEY WORDS: cytochrome c; electromigration; iontophoresis; protein delivery; skin permeation.

INTRODUCTION

The physicochemical properties of peptides and proteins, namely, high molecular weight, charge and hydrophilicity, severely restrict their uptake by the lipid-rich stratum corneum and limit passive diffusion through the intercellular lipid matrix. However, charge and hydrophilicity facilitate peptide electrotransport through the skin, via primarily aqueous transport pathways, by transdermal iontophoresis (1): a non-invasive technology that uses a mild electric current to increase the mobility of charged molecules across the skin (2,3).

Although there are reports of the iontophoretic enhancement of different peptide hormones with molecular weights (MW) in the 1–6 kDa range including luteinising hormone releasing hormone (4,5), calcitonin (6,7), growth hormone releasing hormone (8), human parathyroid hormone (9) and insulin (10,11), the effect of molecular size and protein structure on iontophoretic transport has not been well characterized. For a series of fluorescently-labeled poly-L-lysines (FITC-PLLs) ranging in MW from 4 to 26 kDa, iontophoresis enhanced the penetration of the 4 kDa analog but did not have any effect on the transport of the larger 26 kDa FITC-PLL (12). The transdermal iontophoretic flux of an unidentified cationic protein ("Protein X") with molecular weight of ~12 kDa at an applied current density of 0.1 $mA.cm^{-2}$ (concentration not given, assayed by radioactive-labelling), was measured to be ~15 $\mu g.cm^{-2}.h^{-1}$ (13). It was subsequently reported that "Protein X" was in fact Cytochrome c (14). Comparison of the normalized iontophoretic fluxes of a series of negatively charged compounds across hairless mouse skin (HMS) *in vitro* as a function of MW suggested that electrotransport decreased with increasing molecular size (15). It has also been proposed that large, bulky ions will only carry a small fraction of the

[1] School of Pharmaceutical Sciences, University of Geneva & University of Lausanne, 30 Quai Ernest Ansermet, 1211 Geneva, Switzerland.
[2] "Pharmapeptides", Centre Interuniversitaire de Recherche et d'Enseignement, 74160 Archamps, France.
[3] División de Estudios de Posgrado (Tecnología Farmacéutica), Facultad de Estudios Superiores Cuautitlán, Universidad Nacional Autónoma de México, Av. 1° de Mayo S/N Cuautitlán Izcalli, 54704 Estado de México, Mexico.
[4] Present address: Triskel Integrated Services SA, 4 rue des Terreaux-du-Temple, 1201 Geneva, Switzerland.
[5] To whom correspondence should be addressed. (e-mail: yogi.kalia@pharm.unige.ch)

ABBREVIATIONS: ACE, acetaminophen; Cyt c, cytochrome c; CZE, capillary zone electrophoresis; EM, electromigration; EO, electroosmosis; $J_{EM,\ Cyt\ c}$, flux due to electromigration of Cyt c; $J_{EO,\ Cyt\ c}$, flux due to electroosmosis of Cyt c; $J_{tot,\ Cyt\ c}$, total steady-state flux of Cyt c; V_w, convective solvent flow.

0724-8741/07/0700-1360/0 © 2007 Springer Science + Business Media, LLC

charge passing across the skin and hence can only be transported by electroosmosis; thus, as cation MW increases, there will be a transition in the dominant iontophoretic transport mechanism from electromigration (EM) to electro-osmosis (EO) (16).

Our recent work has demonstrated that the ratio of charge to MW, which determines electric mobility, is a key parameter in governing iontophoretic peptide transport rates (17). A comparison of lysine and H-Lys-Lys-OH transport revealed that the 2-fold increase in molecular weight (149 and 274 Da) was compensated by doubling the charge ($J_{tot} = 225 \pm 48$ and 218 ± 40 nmol. $cm^{-2}.h^{-1}$, respectively); in contrast, H-His-Lys-OH, with approximately the same molecular weight as H-Lys-Lys-OH but unit charge (at pH 7.4), had a significantly lower flux (107 ± 29 $nmol.cm^{-2}.h^{-1}$). For dipeptides of a given MW, e.g., H-Tyr-D-Arg-OH (MW = 337 Da, +1) and H-Tyr-D-Arg-NH_2 (MW = 336 Da, +2), the increment in charge led to a significant difference in total flux (150 ± 26 and 237 ± 35 $nmol.cm^{-2}.h^{-1}$, respectively). Furthermore, we have also shown that there is a correlation between EM flux across skin and electrophoretic mobility measured by capillary zone electrophoresis (CZE): increasing mobility resulted in increased EM flux for a series of small molecules that did not interact with the skin transport pathway (18). Thus, it seemed appropriate to investigate whether the principle of using molecular charge to facilitate electrotransport by compensating for molecular weight, and hence increasing electric mobility, could be extended to proteins. If this were the case, it would obviously increase the range of molecules that could be considered as candidates for non-invasive iontophoretic administration across the skin.

Horse heart cytochrome c (Cyt c, Fig. 1) was chosen as a model protein (19). It has a compact globular structure consisting of a single polypeptide chain, which houses a central heme group. It has a MW of ~12.4 kDa, an isoelectric point of 10.2, (the protein contains a total of 21 amino acids with positively charged side-chains (Arg and Lys), 12 amino acids with negatively charged side-chains (Asp and Glu), and three His residues. The aim of the present work was (1) to evaluate the feasibility of delivering intact Cyt c across the skin by transdermal iontophoresis, (2) to demonstrate that electromigration and not electroosmosis was the key transport mechanism and (3) to investigate the effect of experimental variables including protein concentration, applied current density, and the presence of competing charge carriers, on iontophoretic transport rates in order to establish whether these factors, which govern small molecule delivery, affected macromolecular transport in the same way.

MATERIALS AND METHODS

Materials

Horse heart Cyt c (MW ~12.4 kDa; charge ~+9 at pH 8.2), acetaminophen (ACE), sodium chloride, di-sodium hydrogen phosphate, potassium dihydrogen phosphate, trifluoroacetic acid (TFA), and citric acid were all purchased from Fluka (Saint Quentin Fallavier, France). Silver wire and silver chloride used for the fabrication of electrodes and acetonitrile (Acetonitrile Chromasolv® HPLC, gradient grade) were purchased from Sigma-Aldrich (St. Quentin Fallavier, France). Silicon tubing (3.2 mm ID, 6 mm OD, 1 mm wall) for collecting samples and PVC tubing (3 mm ID, 5 mm OD, 1 mm wall) used to prepare salt bridge assemblies were obtained from Fisher Bioblock Scientific S.A. (Illkirch, France). All solutions were prepared using deionised water (resistivity > 18 MΩ.cm). All other chemicals were at least of analytical grade.

Protein Stability

Solution Stability. The stability of Cyt c in solution as a function of temperature was investigated by periodic sampling of solutions (10 and 100 $\mu g.ml^{-1}$ in phosphate buffered saline pH 7.4 (PBS); 16.8 mM Na_2HPO_4 / 1.4 mM KH_2PO_4 / 136.9 mM NaCl) in order to ensure the integrity of the protein in the putative receptor phase for a period of 48 h. Cyt c formulations were stored at 5 and 25°C. Samples were assayed after 8, 24 and 48 h and were run twice.

Electrical Stability. The impact of electrical current on the stability of Cyt c solutions was evaluated prior to the iontophoretic permeation studies. 5 ml of unbuffered protein solution (8.7 $mg.ml^{-1}$ (0.7 mM), typical concentration for the permeation studies, pH 8.2) was subjected to a current density of 0.5 $mA.cm^{-2}$ using salt bridges (20). Samples were collected and analysed every hour for a period of 8 h. Experiments were performed in triplicate.

Stability in the Presence of Skin. The influence of porcine ear skin on Cyt c stability in solution was assessed by preparing *(a)* 1 $mg.ml^{-1}$ Cyt c in 10 mM NaCl (pH 8.2) and *(b)* 100 $\mu g.ml^{-1}$ Cyt c in PBS at pH 7.4. Dermatomed epidermal and dermal skin surfaces were placed in contact with solutions *(a)* and *(b)*, respectively during 8 h. Samples were evaluated separately and experiments were performed in triplicate.

Iontophoretic Permeation

Protocol. Porcine ears were obtained from a local abattoir (STAC, Chambery, France). The skin was excised (thickness 750 μm) with an electro-dermatome (Zimmer, Etupes, France), wrapped in Parafilm ^{PM} and stored at −20°C for a maximum period of 2 months. Dermatomed skin was clamped in three-compartment vertical flow-through diffusion cells (area 0.85 cm^2). The anode (containing PBS buffer at pH 7.4) was isolated from the donor solution via a salt bridge (SB) assembly (3% agarose in 0.1 M NaCl) to minimize the effect of competing ions (20). After a 40 min equilibration period with PBS, 1 ml of unbuffered peptide solution containing Cyt c (0.7 mM, pH 8.2) and ACE (15 mM) was placed in the donor compartment. ACE was used to report on the electroosmotic solvent flow (20). The cathodal and receptor compartments were filled with 1 and 6 ml of PBS (pH 7.4), respectively. A syringe pump (model SP220IZ, WPI, Sarasota, FL) generated a continuous flow of buffer solution (1 $ml.h^{-1}$) through the receiver compartment, and samples were collected hourly from the second hour onwards. Constant current densities of 0.15, 0.3 and 0.5 $mA.cm^{-2}$ were applied for 8 h via Ag/AgCl electrodes connected to a power supply (Kepco® APH 1000M, Flushing, NY).

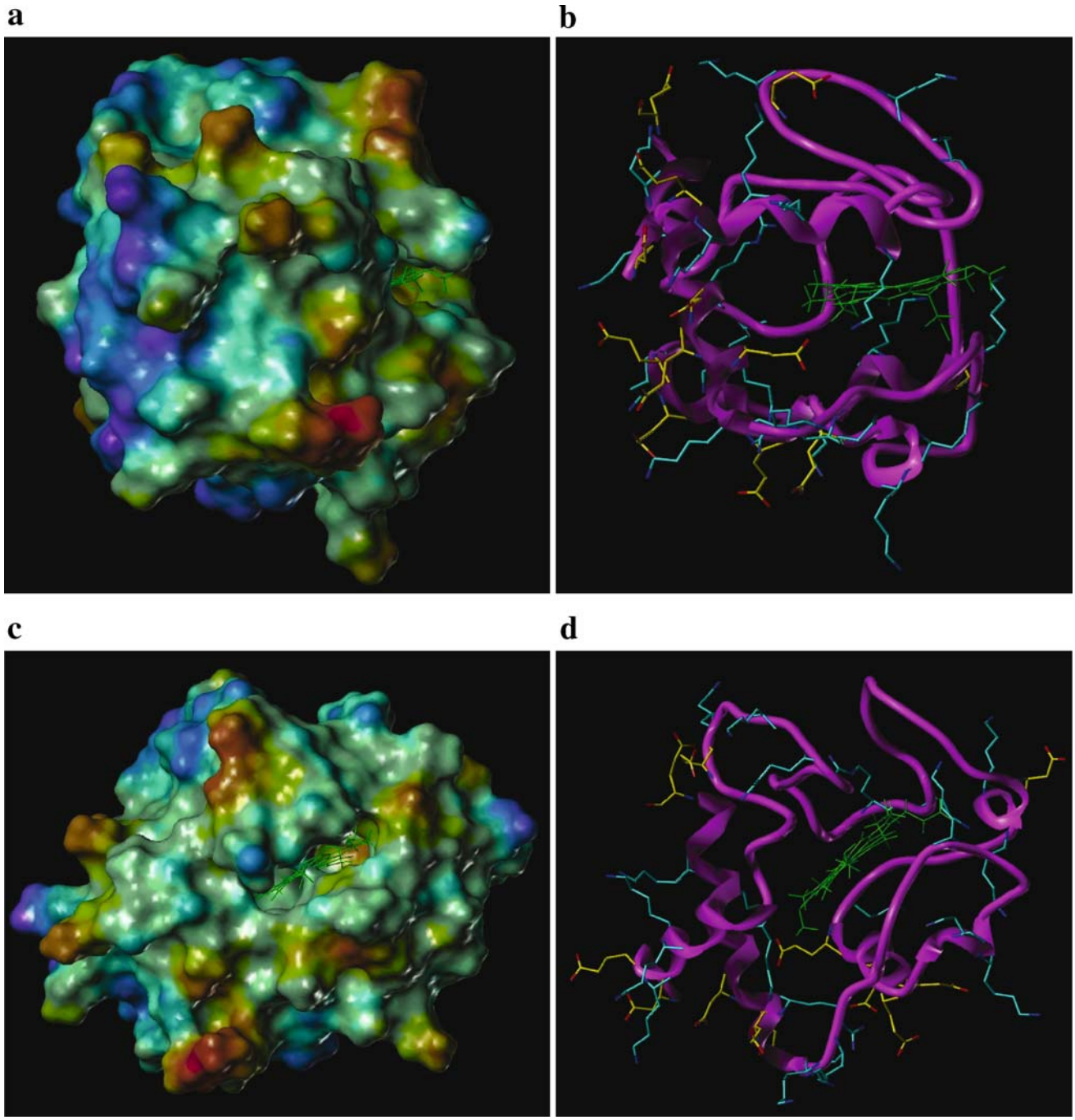

Fig. 1. Three-dimensional structure of horse heart Cytochrome c (Cyt c; 12.4 kDa, +9 at pH 8.2); the compact globular structure of the protein is readily discernable (the heme group is shown *in green*). **a** and **c** present different views of the solvent accessible (Connolly) surface showing the electrostatic potential distribution across the molecular surface (*red and blue colours* represent regions of high positive and negative charge density, respectively). Distinct areas of positive and negative charge density can be clearly seen in (**a**); a more homogenous surface charge distribution is shown in (**c**). The corresponding views of the protein backbone, tertiary structure and the distribution of positively (Arg and Lys; cyan) and negatively (Asp and Glu; *yellow*) charged amino acid residues are shown in (**b**) and (**d**). The charged amino acids are predominantly located on the protein surface; the presence of negative charge density may inhibit electrostatic interactions between Lys or Arg residues and negative charge sites in the transport pathway (see "Discussion"); thus, reducing the effect of Cyt c passage on skin permselectivity. The 1hrc pdb file (Author Y Luo and G.D. Brayer (19) was downloaded from http://www.rcsb.org. Molecular modelling and graphics were done using SYBYL® 7.1 (Tripos Inc., 1699 South Hanley Rd., St. Louis, Missouri, 63144, USA).

Effect of Concentration. This was investigated in a separate study, where the donor compartment contained a solution comprising 0.35 mM Cyt c and 15 mM ACE. All other aspects of the protocol were the same as those outlined above.

Effect of Competing Ions. Cyt c solution (0.7 mM) was prepared using PBS buffer at ~pH 8.2 in order to investigate the effect of competing cations. These formulations contained ~170 mM Na^+; transport experiments were conducted at a current density of 0.5 mA.cm^{-2}.

The permeation experiments were performed in at least quadruplicate.

HPLC Analysis

A P680A LPG-4 pump equipped with an ASI-100 auto sampler and a UV-Vis detector (UVD 170/340-U) (Dionex, Voisins LeBretonneux, France) was used to quantify Cyt c. Isocratic separation was performed using a 150 mm × 4.6 mm base stable (from pH 2.0–10) column packed with 5 μm C4 silica reversed-phase particles (Phenomenex, Le Pecq, France). The flow-rate and the injection volume were 1.0 ml.min^{-1} and 10–100 μl, respectively; the column temperature was kept at 30°C using a thermostat (TCC-100, Dionex GmbH, Germany). The mobile phase consisted of 66.0% of the aqueous component (0.1% TFA (v/v) in water pH 2.0) and 34.0% of the organic phase (0.1% TFA (v/v) in a 90:10 mixture of MeCN: water) (adapted from (21)). The column was equilibrated for at least 1 h. All solvents were filtered (0.45 μm pore size nylon membrane filter) and degassed prior to use. The UV absorbance at 400 nm was used to detect the protein. The limit of quantification (LOQ) and detection (LOD) were 190.0 and 62.7 ng, respectively. ACE was assayed separately using a Lichrospher® 100 RP-8 5 μm reversed-phase column (125 × 4 mm; Lichrocart) with pre-filter. The mobile phase comprised 88% citrate buffer 40 mM (pH = 3.0) and 12% MeCN. Fresh buffer solution was prepared daily. The flow rate and the injection volume were 1.0 ml.min^{-1} and 10–100 μl, respectively. All the samples were diluted (1:20) prior to the analysis. ACE was detected by its UV absorbance at 243 nm. The LOQ and LOD were 8.9 and 2.9 ng, respectively.

The amount of Cyt c retained in the skin samples during the iontophoretic permeation experiments at 0.3 and 0.5 mA.cm^{-2} was estimated by skin extraction using the HPLC mobile phase as the extraction medium. Five and ten ml of mobile phase comprising 66.0% of the aqueous phase (0.1% TFA (v/v) in water pH 2.0) and 34.0% of the organic phase (0.1% TFA (v/v) in a 90:10 mixture of MeCN: water 90:10) were used for the samples from the experiments at 0.3 and 0.5 mA.cm^{-2}, respectively. The skin samples were cut and immersed in the solvent for 4 h under constant stirring at ambient temperature. The samples were analysed using HPLC and the experiments were performed in at least triplicate.

Theory

Estimation of EM and EO Contributions

The total iontophoretic flux ($J_{tot,\ Cyt\ c}$) of Cyt c, assuming negligible passive diffusion, is the sum of the fluxes dues to electromigration ($J_{EM,\ Cyt\ c}$) and electroosmosis ($J_{EO,\ Cyt\ c}$) and is given by Eq. 1 (22):

$$J_{tot,Cytc} = J_{EM,Cytc} + J_{EO,Cytc} = \left(\frac{i_d}{F} \bullet \frac{u_{Cytc}}{\sum_{1}^{i} z_i u_i c_i} + V_W \right) c_{Cytc} \quad (1)$$

$J_{EM,Cyt\ c}$ is related to the current density (i_d), by Faraday's constant (F) and is proportional to $u_{Cyt\ c}$ and $c_{Cyt\ c}$, the mobility and concentration, respectively of the protein in the membrane; z_i, u_i, and c_i refer to the corresponding values for the other charge carriers in the system. The EO contribution, $J_{EO,\ Cyt\ c}$, is proportional to the volume flow induced by the applied potential gradient and is the product of the solvent permeability coefficient (V_W) and the protein concentration, $c_{Cyt\ c}$; the former can be estimated from Eq. 2 (20):

$$V_W = \frac{J_{ACE}}{c_{ACE}} \quad (2)$$

where J_{ACE} is the ACE flux and c_{ACE} is its concentration in the donor compartment.

Inhibition Factor

For each experiment, an inhibition factor (IF) was calculated using the following equation:

$$IF = \frac{V_{W,control}}{V_{W,Cytc}} \quad (3)$$

where $V_{w,control}$ is the solvent permeability coefficient calculated during 8 h of iontophoresis in the absence of protein, and $V_{w,Cyt\ c}$ is the corresponding value when Cyt c was simultaneously iontophoresed.

Statistical Analysis

Data were expressed as mean ± S.D. Outliers, determined using the *Grubbs test* (23), were discarded. The results were evaluated statistically using analysis of variance (ANOVA); *Student's t-test* was used to compare two data sets. The level of significance was fixed at $p < 0.05$.

RESULTS

Cytochrome c Stability

HPLC analysis confirmed that Cyt c response (retention time, peak width, and symmetry) was unaffected by current application (0.5 mA.cm^{-2}) for 8 h. Furthermore, Cyt c was also stable in the presence of both epidermal and dermal skin samples (*Student's t-test*, $p < 0.05$). Similarly, the solution stability experiments carried out at different temperatures also showed that the protein was unchanged; statistical tests did not show any significant difference between the samples stored for 48 h at 5

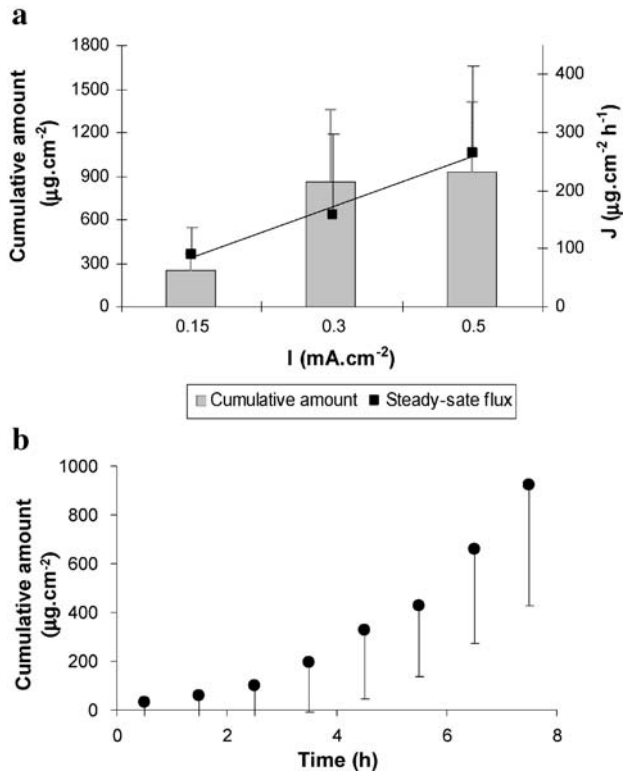

Fig. 2. **a** Cumulative amounts permeated and steady-state fluxes (J_{tot}) of Cyt c across porcine skin during 8 h of transdermal iontophoresis at 0.15, 0.3 and 0.5 mA.cm^{-2}. (Mean±SD) ($n \geq 5$) and **b** Cumulative Cyt c permeation as a function of time during 8 h iontophoresis at 0.5 mA.cm^{-2}. (Mean±SD) ($n = 12$).

and 25°C. These results suggested that Cyt c would be stable under the conditions to be used for the permeation experiments.

Iontophoretic Delivery

In the first series of Cyt c transport experiments, the impact of increasing current density from 0.15 to 0.5 mA.cm^{-2} was tested using a protein concentration of 0.7 mM. The cumulative amount permeated and the iontophoretic flux at 0.15, 0.3 and 0.5 mA.cm^{-2} are shown in Fig. 2. The measured steady-state fluxes were 90.91 ± 45.07, 157.77 ± 140.13, and 265.15 ± 149.05 µg.cm^{-2}.h^{-1}, respectively. A two-fold increase in applied current resulted in an approximately proportional flux enhancement; however, Cyt c flux at 0.3 and 0.5 mA.cm^{-2} was not significantly different (*Student t test, $p < 0.05$*). From Eq. 1, it is clear that the flux due to electromigration, J_{EM}, should increase with the applied current and this is the case for several small molecules and some peptides, both *in vitro* and *in vivo* (24–27). It has been suggested that at high current densities, the iontophoretic response saturates and once a limiting transport number is achieved, further increase in current has no effect (28). Similarly, the cumulative permeation of Cyt c at 0.3 and 0.5 mA.cm^{-2} was greater than that at 0.15 mA.cm^{-2}. Figure 3 shows the amounts of Cyt c extracted from the skin after completion of the permeation experiments. Although greater amounts of protein were recovered from the skin samples used in the experiments at 0.3 mA.cm^{-2} (2,060.82 ± 367.53 µg.cm^{-2}) than at 0.5 mA.cm^{-2} (951.55 ± 201.08 µg.cm^{-2}); the sum of the amounts extracted and permeated at the two current densities was not statistically different.

Co-iontophoresis of ACE enabled the estimation of the contributions of EM, EO and the calculation of an electroosmotic inhibition factor (IF) (Table I). Control values for ACE flux in the absence of Cyt c were determined independently with applied current densities of 0.15, 0.3 or 0.5 mA.cm^{-2}. Calculation of the EO contribution and subtraction from the total flux showed that EM was the dominant mechanism, accounting for ~90% of total Cyt c delivery. A two-fold increase (0.15–0.3 mA.cm^{-2}) in current produced an approximately proportional increase in the EM and EO contributions. Inhibition of ACE transport, caused by reduction of convective solvent flow was only noticeable at the highest current density (0.5 mA.cm^{-2}), with an IF ~5; however, this did not have a significant impact on Cyt c transport since EM was by far the dominant transport mechanism (Fig. 4). Moreover, although significant amounts of Cyt c were extracted from the skin following iontophoresis at 0.3 mA.cm^{-2}, there was no concomitant effect on ACE transport and hence convective solvent flow (as evidenced by IF ~1, Table I). Thus, Cyt c accumulation in the membrane at 0.3 mA.cm^{-2} was not in itself a sufficient condition for significant EO inhibition; this may point to Cyt c aggregation or to the presence of intermolecular interactions that do not involve the fixed negative charges responsible for skin permselectivity.

The effect of concentration on the iontophoretic transport of Cyt c was examined in the second series of experiments. Figure 5 shows that increasing the donor concentration from 0.35 to 0.7 mM Cyt c, in the absence of competing ions, affected neither the cumulative permeation (594.0 ± 257.4 and 923.0 ± 496.1 µg.cm^{-2}, respectively; *t*-test, $p < 0.05$) nor the flux (J_{tot} = 182.8 ± 56.8 and 265.2 ± 149.1 µg.cm^{-2}.h^{-1}, respectively; *t*-test, $p < 0.05$). Similarly, ACE transport was not affected by the two-fold difference in donor concentration and the solvent permeability coefficient, V_W, was effectively unchanged ((27.9 ± 19.0) and (18.4 ± 10.8) 10^{-4}cm.h^{-1} respectively) at the two concentrations. At the lower concentration, EM was again the dominant transport mechanism governing the iontophoretic transfer of Cyt c, accounting for >90% of total flux; thus, there was no change in the relative contributions of EM and EO to overall elec-

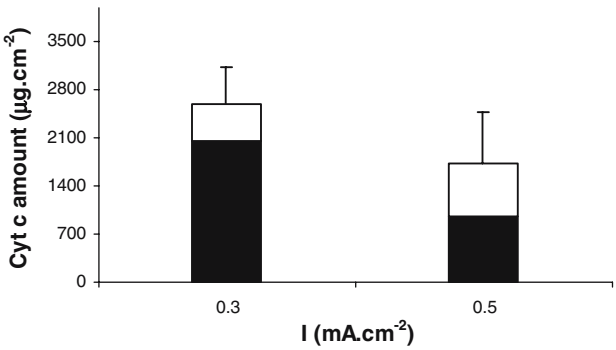

Fig. 3. Effect of current density on the cumulative amount of Cyt c permeated across porcine skin (*open square*) and retained within the membrane (*closed square*). (Mean ± SD) ($n \geq 3$).

Table I. Iontophoretic Transport Kinetics of Horse Heart Cytochrome C and the Relative Contributions of Electromigration and Electroosmosis

I (mA cm^{-2})	J_{tot} (μg cm^{-2} h^{-1})	J_{EM} (μg cm^{-2} h^{-1})	J_{EO} (μg cm^{-2} h^{-1})	$10^4 V_{W,\ Cyt\ c}$ (cm h^{-1})	$10^4 V_{W,\ control}$ (cm h^{-1})	IF
0.15	90.91 ± 45.07	82.00	8.91	8.61 ± 4.91	16.61 ± 7.45	1.93 ± 1.40
0.30	157.77 ± 140.13	137.93	19.84	20.94 ± 7.92	21.40 ± 2.73	1.02 ± 0.47
0.50	265.15 ± 149.05	248.71	16.44	18.41 ± 10.81	90.72 ± 29.34	4.93 ± 3.08

($n \geq 4$)
I: Current density, J_{EM}: Electromigration contribution, J_{EO}: Electroosmotic contribution, J_{tot}: Total steady-state flux, $V_{W,Cyt\ c}$: solvent permeability coefficient in the presence of Cyt c, $V_{W,\ control}$: solvent permeability coefficient, *IF*: Inhibition factor (calculated according to Eq. 3).

trotransport. (*Student's t-test, $p < 0.05$*). Under the experimental conditions used, Cyt c was the sole cation in the anodal formulation; the majority of the charge transfer was due to Cl^- ions moving from the receiver compartment towards the anode. The electrodiffusion model developed by Kasting and Keister (28) suggests that, in the absence of competing cations, iontophoretic flux is independent of concentration and dependent only on the ratio of diffusivities (or mobilities) of the cation and the main counterion (usually Cl^-) arriving from beneath the skin.

The addition of buffer or an increase in the ionic strength of the formulation by the addition of background electrolyte increases competition between charge carriers and generally decreases iontophoretic drug flux (29–31). The effect of Na^+ on the iontophoretic transport of Cyt c (0.7 mM) was confirmed by formulating the protein in PBS (pH 8.2). The estimated flux and the transport efficiency as a function of experimental conditions are shown in Fig. 6. The presence of ~170 mM Na^+ resulted in a 3.9-fold decrease in J_{tot} (67.5 ± 15.7 μg.cm^{-2}.h^{-1}) which was entirely due to a decrease in the EM contribution to Cyt c electrotransport. Calculation of the Cyt c transport number for the two experimental conditions showed that inclusion of Na^+ (at >200-fold excess as compared to the protein) caused Cyt c transport efficiency to decrease from 0.048 to 0.010%. Although the presence of competing ions resulted in a significant decrease in Cyt c delivery, it did not impact on EO flow.

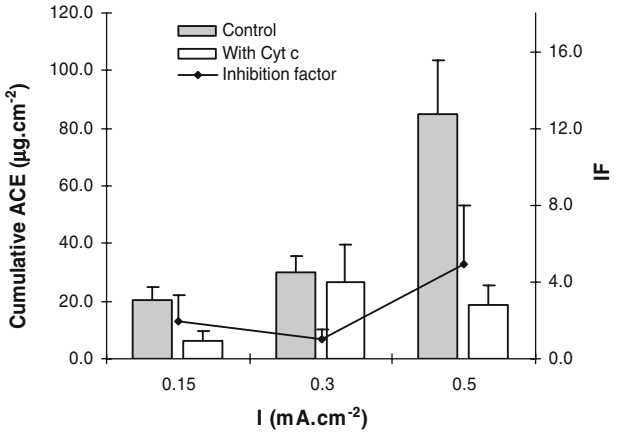

Fig. 4. Cumulative amount of acetaminophen (ACE) delivered across the skin after 8 h of transdermal iontophoresis at 0.15, 0.3 and 0.5 mA.cm^{-2} in the presence and in the absence of Cyt c. The inhibition factor (IF) is calculated according to Eq. 3. (Mean±SD) ($n \geq 4$).

DISCUSSION

Electric Mobility Governs Cyt c Electrotransport

The relative contributions of EM and EO (Table I) to Cyt c electrotransport across the skin show that EM accounted for ~90% of total delivery despite the molecular weight of the protein; providing clear evidence that EO does not per se govern peptide or protein iontophoretic transport rates (27). The dominant transport mechanism will depend on the physicochemical properties of the macromolecule, in particular, its electric mobility. Figure 7 shows the normalized steady state electromigratory flux (J_{EM}^{norm}) of lidocaine, propranolol, quinine and a series of lysine- and tyrosine-containing dipeptides as a function of electrophoretic mobility (adapted from (18)). Inclusion of the corresponding normalized flux for Cyt c using the same current density and similar conditions (0.5 mA.cm^{-2}, 0.7 mM, PBS pH 8.2) and assuming a mobility of 4×10^{-5} cm^2.V^{-1}.s^{-1} (32) shows that despite its much greater MW, Cyt c electromigration displays the same correlation with its electrophoretic mobility ($J_{EM}^{norm} = 92.76u_i + 0.0031$, $r^2 = 0.97$).

High molecular weight peptides and small proteins with multiple exposed charged amino acid side chains or available hydrophobic surfaces may interact strongly with structures in

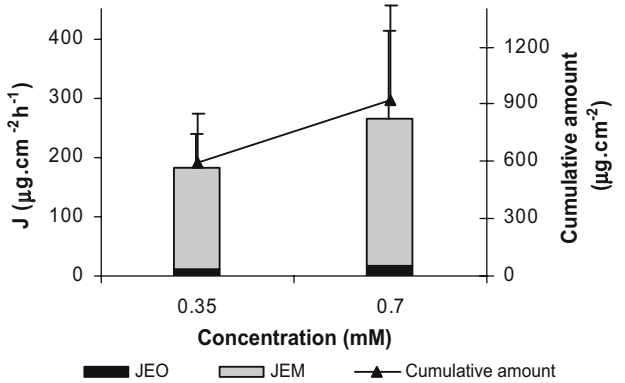

Fig. 5. Iontophoretic transport of Cyt c at constant current (0.5 mA.cm^{-2}) was independent of donor concentration (0.35 and 0.7 mM Cyt c) in the absence of competing ions. (Mean ± SD) ($n \geq 6$).

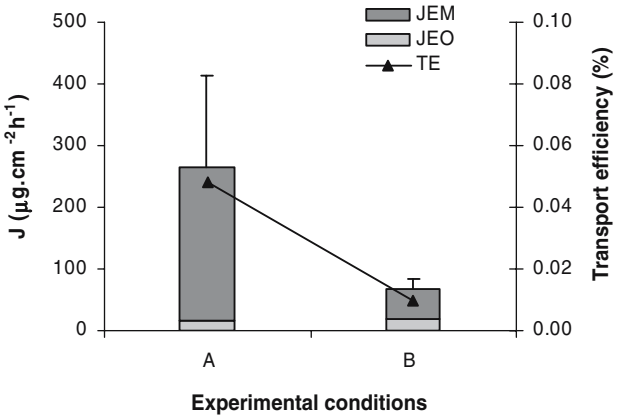

Fig. 6. The impact of ion competition on Cyt c electrotransport at 0.5 mA.cm^{-2}. Formulation in PBS containing ~170 mM Na^+ caused a significant decrease in flux. Electromigration contribution (*EM*); Electroosmosis contribution (*EO*); Transport efficiency (*TE*). Experimental setup: *A* = with salt bridge; *B* = without salt bridge. (Mean±SD) ($n \geq 5$).

the transport pathway, either through electrostatic or van der Waals' type interactions. If these associations are accompanied by neutralization of the fixed negative charges in the skin, this will result in reduced convective flow. These interactions with the biological transport pathway will also reduce the reliability of electrophoretic mobility as a predictor for peptide or protein electrotransport. Increasing current density causes more protein to be transported into the skin and increases the likelihood of interaction: for Cyt c, inhibition of skin permselectivity was only significant at a current density of 0.5 mA.cm^{-2}. However, since EM was by far the dominant transport mechanism it had negligible impact on total flux.

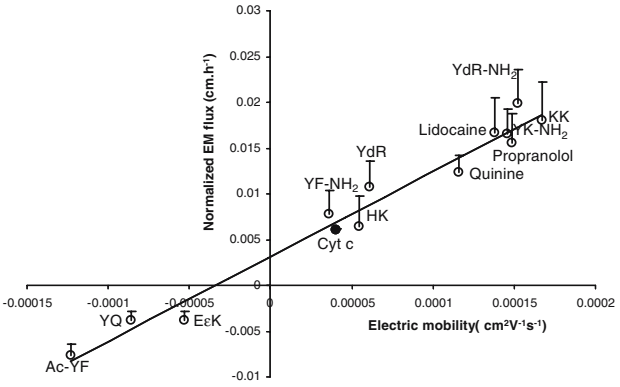

Fig. 7. Correlation between normalized EM flux (J_{EM}^{norm}, cm.h^{-1}) and electrophoretic mobility (u_i, cm^2.V^{-1}.s^{-1}) for a series of small molecules and dipeptides (hollow circles) (10 mM, 0.5 mA.cm^{-2}, adapted from (18)). The normalized EM flux of Cyt c (0.7 mM buffered in PBS, 0.5 mA.cm^{-2}) shows the same dependence on its electric mobility (average value of 4×10^{-5} cm^2.V^{-1}.s^{-1} (32)) (*filled circle*); for example, its mobility is approximately four-fold less than that of YdR-NH_2 and it shows a corresponding four-fold lower normalized flux. As for the smaller molecules and dipeptides, under these iontophoretic conditions, Cyt c does not interact with the transport pathway in the skin; hence, its electrophoretic mobility as measured by CZE is a good predictor of the flux due to electromigration. ($J_{EM}^{norm} = 92.76u_i + 0.0031$, $r^2 = 0.97$).

Feasibility of Delivering Small Proteins by Transdermal Iontophoresis

Comparison of our results with those of "Protein X" (13) is difficult, given the lack of experimental details; however, assuming similar protein concentrations in the respective formulations (and the presence of competing ions), then the current-normalized fluxes are similar (~150 µg.mA.h^{-1} for "Protein X" and ~135 µg.mA.h^{-1} for Cyt c in the present study—0.7 mM, 0.5 mA.cm^{-2}, PBS pH 8.2).

Laser scanning confocal microscopy studies using FITC-labelled poly-L-lysines with molecular weights of 4, 7 and 26 kDa showed that although iontophoresis (0.5 mA.cm^{-2} at 0.05 mM polypeptide) enhanced delivery of the 4 kDa derivative it had little or no effect on the transport of the larger species; after 8 h iontophoresis at 0.5 mA.cm^{-2}, cumulative permeation of the 4 and 7 kDa poly-L-lysines was 3.84 ± 1.48 and 0.44 ± 0.12 µg, respectively (12). Iontophoresis of 2.7, 8.2 and 20 kDa poly-L-lysines (0.5 mA.cm^{-2} and 3.7, 1.2 and 0.5 mM, respectively) decreased skin permselectivity as

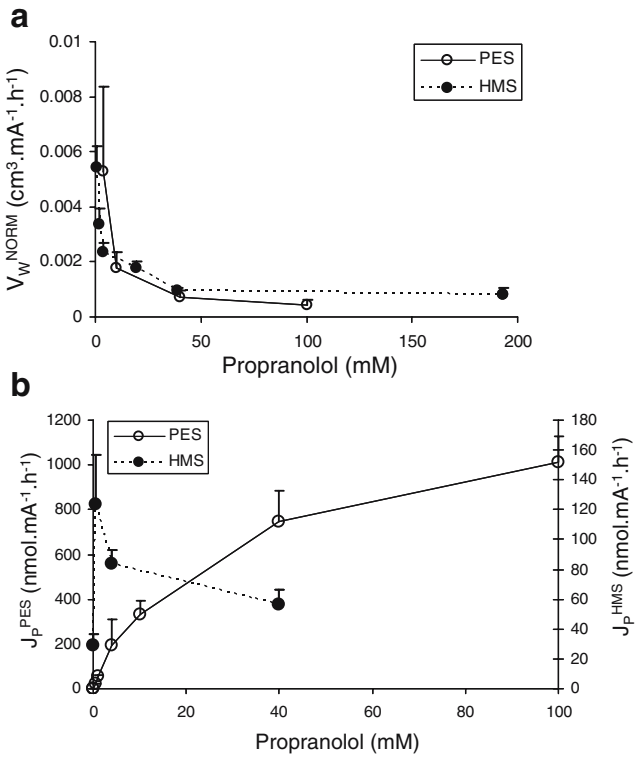

Fig. 8. **a** Variation of the current-normalized convective solvent flow across porcine ear skin (*PES*) and hairless mouse skin (*HMS*) in the presence of propranolol as a function of drug concentration in the formulation. A similar exponential decrease is observed with both membranes. **b** Variation of the current-normalized propranolol flux across *PES* and *HMS* as a function of drug concentration is strikingly different. Although a "plateau" is observed with *PES* as the concentration increases, the flux across *HMS* passes through a sharp maximum at a low concentration (0.4 mM). Thus, the nature of the biological barrier can have a significant on molecular electrotransport. Data from (35) and (36).

measured by mannitol flux (by up to 30-fold in the case of the 20 kDa derivative (33)): the pronounced EO inhibition suggesting the presence of the polypeptide in the transport pathway. These poly-L-lysine results are very different to those observed with Cyt c both in terms of cumulative protein delivery (784.52 ± 421.64 μg after 8 h at 0.5 $mA.cm^{-2}$) and the effect on convective solvent flow (only a ~5-fold decrease in ACE transport under the same conditions). Furthermore, for comparison, PL_{83}, a poly-L-lysine containing 83 Lys residues, with a molecular weight of ~12.5 kDa, is reported to have an electrical mobility of 16×10^{-5} $cm^2.V^{-1}.s^{-1}$ (34), which is four times greater than that of Cyt c; therefore, why does the latter show superior iontophoretic transport kinetics?

The poly-L-lysine experiments were conducted using hairless mouse skin (HMS) whereas the iontophoretic transport of Cyt c was investigated across porcine ear skin. The nature of the membrane can have a significant impact on iontophoretic drug transport rates. For example, although the variation of the current-normalized convective solvent flow across both HMS and porcine ear skin (PES) as a function of propranolol concentration, as reported by mannitol flux, is similar (Fig. 8a), propranolol transport kinetics are completely different (Fig. 8b) (3,35,36). Thus, although increasing propranolol concentration in the formulation has a similar effect on skin permselectivity in both membranes, the presence of drug–drug or drug-pathway interactions causes current-normalized propranolol flux across HMS to decrease sharply after reaching a maximum at 0.4 mM. By analogy, poly-L-lysines may have a greater propensity to bind to structures along the transport route or to self-aggregate during iontophoresis across HMS than is the case for Cyt c in PES.

Cyt c and the poly-L-lysines also have very different structures and solution conformations. Under physiological conditions, poly-L-lysine has a dynamic random coil structure in solution; in contrast, Cyt c possesses a compact globular structure ($2.5 \times 2.5 \times 3.7$ nm, (37)) with a well-defined three-dimensional conformation containing three major and two minor helices separated by strands with more random structure, folded around a heme group (19) (Fig. 1). A 20 kDa poly-L-lysine contains ~130 lysine residues in a polypeptide chain with a random coil structure. The Lys side-chains will be extensively exposed to the solution so that the side chain ε-NH_2 group can interact with anions or form hydrogen-bonds with surrounding water molecules—these groups will also be predisposed to interacting with accessible sites of negative charge density present in the iontophoretic transport pathway. Although Cyt c is rich in Arg and Lys residues (~21 residues), that are also found at the protein surface, solvent-accessible and whose side-chains show considerable flexibility (Fig. 1b and d), the more rigid three-dimensional structure of the protein backbone restricts the number of possible side-chain-membrane interactions. Furthermore, the presence of surface negative charges (due to Asp and Glu) may also hinder interaction with negative sites within the membrane (Fig. 1a and c). Thus, Cyt c would have a lower propensity to interact with the membrane and its electrotransport less likely to modulate skin permselectivity.

With respect to the feasibility of delivering small proteins through the proposed transport pathways in the skin, analysis of the results from streaming potential measurements using excised human cadaver abdominal skin, using a capillary pore model, suggested the presence of nanopores with a Gaussian size distribution and a mean radius on the order of ~20 nm (38). The pore diameter would be sufficient to enable passage of a small globular protein such as Cyt c. More recently, scanning electrochemical microscopy (SECM) studies into the electroosmotic transport of acetaminophen across full-thickness human cadaver skin demonstrated that electroosmotic phenomena occurred in pores, tentatively identified as skin appendageal structures, much larger than nanopores (39). Conversion of the SECM tip current to a concentration followed by fitting to an appropriate mathematical model, enabled estimation of the pore radius (~35 μm); obviously, protein transport through these appendageal structures would be entirely feasible. In contrast, earlier studies with HMS suggested non-appendageal pore radii of 2.7, 1.35 and 0.675 nm for negative, neutral and positive pores, respectively (40). Similarly, a hydrodynamic model developed using rat skin suggested that the pore diameter was ~3.6 nm (41). For these two animal models, the passage of Cyt c through these narrower, non-appendageal channels would probably be hindered—these observations may also partly explain the poly-L-lysine transport results (12,35).

CONCLUSIONS

These results demonstrate the feasibility of delivering significant amounts of Cyt c, a small, highly charged protein, non-invasively across intact skin (~0.9 $mg.cm^{-2}$ over an 8 h period). They also show that Cyt c electrotransport was governed by EM (~90%) and not EO. Furthermore, neither Cyt c permeation nor its accumulation in the skin caused EO inhibition at current densities lower than 0.5 $mA.cm^{-2}$ (indeed, its occurrence at this current density had negligible effect on transport kinetics). Thus, a macromolecule with molecular weight exceeding 12 kDa, possessing a suitable charge:MW ratio (and hence, electric mobility) *and* the appropriate three-dimensional structure can be delivered non-invasively by transdermal iontophoresis. Globular proteins with a compact tertiary structure may be better candidates than highly charged polypeptides with extended random coil structures since the latter may be more prone to interaction with the transport pathway (they may also be more susceptible to enzymatic hydrolysis). Future studies will build upon the findings with this model protein and apply the same principles to the non-invasive delivery of therapeutic proteins across the skin.

ACKNOWLEDGEMENTS

We would like to thank Prof. Leonardo Scapozza and Dr. Shaheen Ahmed for help with the molecular graphics representations of Cytochrome c. J. Cázares Delgadillo acknowledges support from CONACYT (Mexico).

REFERENCES

1. Y. B. Schuetz, P-A. Carrupt, A. Naik, R. H. Guy, and Y. N. Kalia. Structure-permeation relationships for the non-invasive

transdermal delivery of cationic peptides by iontophoresis. *Eur. J. Pharm. Sci.* **29**:53–59 (2006).
2. R. R. Burnette. Iontophoresis. In J. Hadgraft and R. Guy (eds.), *Transdermal Drug Delivery*, Marcel Dekker, New York, 1989, pp. 247–288.
3. Y. N. Kalia, A. Naik, J. Garrison, and R. H. Guy. Iontophoretic drug delivery. *Adv. Drug Deliv. Rev.* **56**:619–658 (2004).
4. M. C. Heit, P. L. Williams, F. L. Jayes, S. K. Chang, and J. E. Riviere. Transdermal iontophoretic peptide delivery: *in vitro* and *in vivo* studies with luteinizing hormone releasing hormone. *J. Pharm. Sci.* **82**:240–243 (1993).
5. J. Raiman, M. Koljonen, K. Huikko, R. Kostiainen, and J. Hirvonen. Delivery and stability of LHRH and Nafarelin in human skin: the effect of constant/pulsed iontophoresis. *Eur. J. Pharm. Sci.* **21**:371–377 (2004).
6. P. Santi, N. M. Volpato, R. Bettini, P. L. Catellani, G. Massimo, and P. Colombo. Transdermal iontophoresis of salmon calcitonin can reproduce the hypocalcemic effect of intravenous administration. *Farmaco* **52**:445–448 (1997).
7. A. Chaturvedula, D. P. Joshi, C. Anderson, R. L. Morris, W. L. Sembrowich, and A. K. Banga. *In vivo* iontophoretic delivery and pharmacokinetics of salmon calcitonin. *Int. J. Pharm.* **297**:190–196 (2005).
8. S. Kumar, H. Char, S. Patel, D. Piemontese, A. W. Malick, K. Iqbal, E. Neugroschel, and Ch. R. Behl. Effect of iontophoresis on *in vitro* skin permeation of an analog of growth hormone releasing factor in the hairless guinea pig model. *J. Pharm. Sci.* **81**:635–639 (1992).
9. Y. Suzuki, K. Iga, Sh. Yanai, Y. Matsumoto, M. Kawase, T. Fukuda, H. Adachi, N. Higo, and Y. Ogawa. Iontophoretic pulsatile transdermal delivery of human parathyroid hormone (1–34). *J. Pharm. Pharmacol.* **53**:1227–1234 (2001).
10. L. Langkjaer, J. Brange, G. M. Grodsky, and R. H. Guy. Iontophoresis of monomeric insulin analogs *in vitro*: effects of insulin charge and skin pretreatment. *J. Control. Release* **51**: 47–56 (1998).
11. O. Pillai and R. Panchagnula. Transdermal iontophoresis of insulin: V. Effect of terpenes. *J. Control. Release* **88**:287–296 (2003).
12. N. G. Turner, L. Ferry, M. Price, C. Cullander, and R. H. Guy. Iontophoresis of poly-L-lysines: the role of molecular weight? *Pharm. Res.* **14**:1322–1331 (1997).
13. R. Haak and S. K. Gupta. Pulsatile drug delivery from electrotransport therapeutic systems. In R. Gurny, H. E. Junginger, and N. A. Peppas (eds.), *Pulsatile Drug Delivery—Current Applications and Future Trends, Wiss*, Verl.-Ges., Stuttgart, 1993, pp. 99–112.
14. P. Green. Iontophoretic delivery of peptide drugs. *J. Control. Release* **41**:33–48 (1996).
15. M. B. Delgado-Charro and R. H. Guy. Iontophoresis of peptides. In Bret Berner and S. M. Dinh (eds.), *Electronically Controlled Drug Delivery*, Vol. 1, CRS, New York, 1998, pp. 129–157.
16. R. H. Guy, Y. N. Kalia, M. B. Delgado-Charro, V. Merino, A. López, and D. Marro. Iontophoresis: electrorepulsion and electroosmosis. *J. Control. Release* **64**:129–132 (2000).
17. N. Abla, A. Naik, R. H. Guy, and Y. N. Kalia. Effect of charge and molecular weight on transdermal peptide delivery by iontophoresis. *Pharm. Res.* **22**:2069–2078 (2005).
18. N. Abla, L. Geiser, M. Mirgaldi, A. Naik, J.-L. Veuthey, R. H. Guy, and Y. N. Kalia. Capillary zone electrophoresis for the estimation of transdermal iontophoretic mobility. *J. Pharm. Sci.* **94**:2667–2675 (2005).
19. G. W. Bushnell, G. V. Louie, and G. D. Brayer. High-resolution three-dimensional structure of horse heart cytochrome c. *J. Mol. Biol.* **214**:585–595 (1990).
20. Y. B. Schuetz, A. Naik, R. H. Guy, E. Vuaridel, and Y. N. Kalia. Transdermal iontophoretic delivery of vapreotide acetate across porcine skin *in vitro*. *Pharm. Res.* **22**:1305–1312 (2005).
21. M. J. Picklo, J. Zhang, V. Q. Nguyen, D. G. Graham, and T. J. Montine. High pressure liquid chromatography quantitation of Cytochrome c using 393 nm detection. *Anal. Biochem.* **276**:166–170 (1999).
22. N. Abla, A. Naik, R. H. Guy, and Y. N. Kalia. Contributions of electromigration and electroosmosis to peptide iontophoresis across intact and impaired skin. *J. Control. Release* **108**:319–330 (2005).
23. J. E. De Muth. *Basic Statistics and Pharmaceutical Statistical Applications*, Marcel Dekker, New York, 1999.
24. D. T. W. Lau, J. W. Sharkey, L. Petryk, F. A. Mancuso, Z. Yu, and F. L. S. Tse. Effect of current magnitude and drug concentration on iontophoretic delivery of octreotide acetate (Sandostatin®) in the rabbit. *Pharm. Res.* **11**:1742–1746 (1994).
25. S. K. Gupta, M. Southam, G. Sathyan, and M. Klausner. Effect of current density on pharmacokinetics following continuous or intermittent input from a fentanyl electrotransport system. *J. Pharm. Sci.* **87**:976–981 (1998).
26. P. Singh, S. Boniello, P. Liu, and S. Dinh. Transdermal iontophoretic delivery of methylphenidate HCl *in vivo*. *Int. J. Pharm.* **178**:121–128 (1999).
27. Y. B. Schuetz, A. Naik, R. H. Guy, E. Vuaridel, and Y. N. Kalia. Transdermal iontophoretic delivery of triptorelin *in vivo*. *J. Pharm. Sci.* **94**:2175–2182 (2005).
28. G. B. Kasting and J. C. Keister. Application of electrodiffusion theory for a homogeneous membrane to iontophoretic transport through skin. *J. Control. Release* **8**:195–210 (1989).
29. W. H. M. Craane-van Hinsberg, L. Bax, N. H. M. Flinterman, J. Verhoef, H. E. Junginger, and H. E. Bodde. Iontophoresis of a model peptide across human skin *in vivo*: effects of iontophoresis protocol, pH and ionic strength on peptide flux and skin impedance. *Pharm. Res.* **11**:1296–1300 (1994).
30. M. F. Lu, D. Lee, R. Carlson, G. S. Rao, H. W. Hui, L. Adjei, M. Herrin, D. Sundberg, and L. Hsu. The effects of formulation variables on iontophoretic transdermal delivery of leuprolide to humans. *Drug Deliv. Ind. Pharm.* **19**:1557–1571 (1993).
31. Y. B. Schuetz, A. Naik, R. H. Guy, and Y. N. Kalia. Effect of amino acid sequence on transdermal iontophoretic peptide delivery. *Eur. J. Pharm. Sci.* **26**:429–437 (2005).
32. G. H. Barlow and E. Margoliash. Electrophoretic behaviour of mammalian-type cytochromes c. *J. Biol. Chem.* **241**:1473–1477 (1966).
33. J. Hirvonen and R. H. Guy. Transdermal iontophoresis: modulation of electroosmosis by polypeptide. *J. Control. Release* **50**:283–289 (1998).
34. R. V. Rice, M. A. Stahmann, and R. A. Alberty. The interaction of lysine polypeptides and bovine plasma albumin. *J. Biol. Chem.* **209**:105–115 (1954).
35. J. Hirvonen and R. H. Guy. Iontophoretic delivery across the skin: electroosmosis and its modulation by drug substances. *Pharm. Res.* **14**:1258–1263 (1997).
36. D. Marro, Y. N. Kalia, M. B. Delgado-Charro, and R. H. Guy. Contributions of electromigration and electroosmosis to iontophoretic drug delivery. *Pharm. Res.* **18**:1701–1708 (2001).
37. I. Ichinose, Y. Hashimoto, and T. Kunitake. Wrapping of biomacromolecule (dextran, amylopectin and horse heart Cytochrome c) with ultrathin silicate layer. *Chem. Lett.* **33**:656–657 (2004).
38. V. Aguilella, K. Kontturi, L. Murtomäki, and P. Ramirez. Estimation of the pore size and charge density in human cadaver skin. *J. Control. Release* **32**:249–257 (1994).
39. O. D. Uitto and H. S. White. Electroosmotic pore transport in human skin. *Pharm. Res.* **20**:646–652 (2003).
40. M. J. Pikal. Transport mechanisms in iontophoresis: I. A theoretical model for the effect of electroosmotic flow on flux enhancement in transdermal iontophoresis. *Pharm. Res.* **7**:118–126 (1990).
41. S. B. Ruddy and B. W. Hadzija. Iontophoretic permeability of polyethylene glycols through hairless rat skin: application of hydrodynamic theory for hindered transport through liquid-filled pores. *Drug Des. Discov.* **8**:207–224 (1992).